Algorithm of the Computer Modelling and a SESANS Setup with Adiabatic RF-Flippers

Kraan, Wicher; Zabenkin, V.N.; Axelrod, LA; Chetverikov, Yu.O.; Grigoriev, SV; Yashina, E.G.; Sumbatyan, A.A.

Algorithm of the Computer Modelling and a SESANS Setup with Adiabatic RF-Flippers[1]

W. H. Kraan[a], *, **V. N. Zabenkin**[b], **L. A. Axelrod**[b], **Yu. O. Chetverikov**[b], **S. V. Grigoriev**[b], **E. G. Yashina**[b], and **A. A. Sumbatyan**[b]

[a] *Interfaculty Reactor Institute, Delft University of Technology, 2629 JB Delft The Netherlands*
[b] *Petersburg Nuclear Physics Institute of National Research Centre "Kurchatov Institute", Gatchina, 188300 Russia*
*e-mail: whkraan@gmail.com
Received February 22, 2017

Abstract—We made software to simulate Larmor precession in a setup for SESANS with adiabatic/RF flippers in magnets, existing at PNPI. The final polarisation of a divergent "ribbon beam" of height 2 cm is calculated as a function of λ. For $\lambda = 6$ Å, flippers 56 cm apart and RF frequency 1 MHz we find spin-echo length $\delta = 0.9$ μm. We show numerically, how λ is converted to δ. Extension to $\delta = 20$ μm is realistic.

1. INTRODUCTION

The last 10 years have seen SESANS as an upcoming technique for investigation of the structure and space distribution of inhomogenieties in (soft) condensed matter, gel-like materials, etc, at a length scale from 100 nm−10 μm [1−3]. This technique gives answers in real space *without* the need of beam collimation, contrary to traditional SANS giving answers in reciprocal space, *with* the need of strong beam collimation.

SESANS is a Neutron-Spin-Echo (NSE) experiment in regions with magnetic field, shaped as *parallellograms* (Fig. 1a). Applying the *Satz* [3]: for neutrons of wavelength λ the precession phase ϕ "collected" along a path of length L through a homogeneous induction B is

$$\phi = cLB\lambda,$$

one can see that the precession phases ϕ_i in NSE-arm 1 *before* ($i = 1$) and arm 2 *after* scattering in sample S ($i = 2$) while a neutron traverses the regions, are:

$$\phi_i = \lambda(cLB + \Gamma\psi_i) \ (i = 1, 2), \tag{1}$$

(the constant $c = 4\pi\mu_n m_n/h^2 = 4.632 \times 10^{14}$ T^{-1} m^{-2} with m_n, μ_n, h neutron mass, magn. moment and Planck's constant, respectively). ψ_i are the angles between the x-axis and the flying directions in the NSE-arms. $\lambda\Gamma\psi_i$ is the angle labeling term. For rectangular field shape ($\theta_0 = 90°$) it is 0 in first order. Γ ($= cBL\cot\theta_0$) is called "labeling coefficient".

Suppose a neutron is scattered by $\psi_2 - \psi_1 = \theta_S$ in the y-direction (Fig. 1a). Then Eq. (1) gives the *offset* from NSE due to this process: $\phi_1 - \phi_2 = \lambda\Gamma\theta_S$. Because the term $cBL\lambda$ cancels, *this is true for any type of NSE-arms* (for example Fig. 1c, discussed below). This scattering process has wave vector transfer $Q_y = \frac{4\pi}{\lambda}\sin(\theta_S/2) \approx 2\pi\sin\theta_S/\lambda$. If we divide Q_y out (saying $\sin\theta_S = \theta_S$), we get a quantity of dimension length:

$$\delta = \lambda\Gamma\theta_S/Q_y = \Gamma\lambda^2/2\pi, \tag{2}$$

called "spin-echo length". δ depends on the setup parameters θ_0 (Fig.1a), L, B and λ. For fields shaped as parallellograms we find $\delta(\theta_0, L, B, \lambda) = [1/(2\pi)] cLB\cot\theta_0\lambda^2$.

The nominator and denominator in (2) don't depend on the specific direction ψ_1 in region 1, nor on the position on the y-axis of the neutron on entering. This means that all neutrons making up a parallel sub-beam of given ψ_i in the *incident* beam and, idem, in the *scattered* beam have the same value for δ. This is the reason why good collimation of the incident and scattered beam is not required to "focus" the setup on a specific value of δ.

In the practice of a SESANS measurement, at *given* setting of δ, one measures the damped oscillating polarisation signal $P(\delta, \Delta\phi)$ after the analyser as a function of the precession phase $\Delta\phi$ collected in a so-called "phasecoil", mounted in one NSE-arm for the purpose to make *offset* from NSE. The polarisation $P(\delta)$ is the maximum amplitude of this signal. Scan-

---

[1] The article is published in the original.
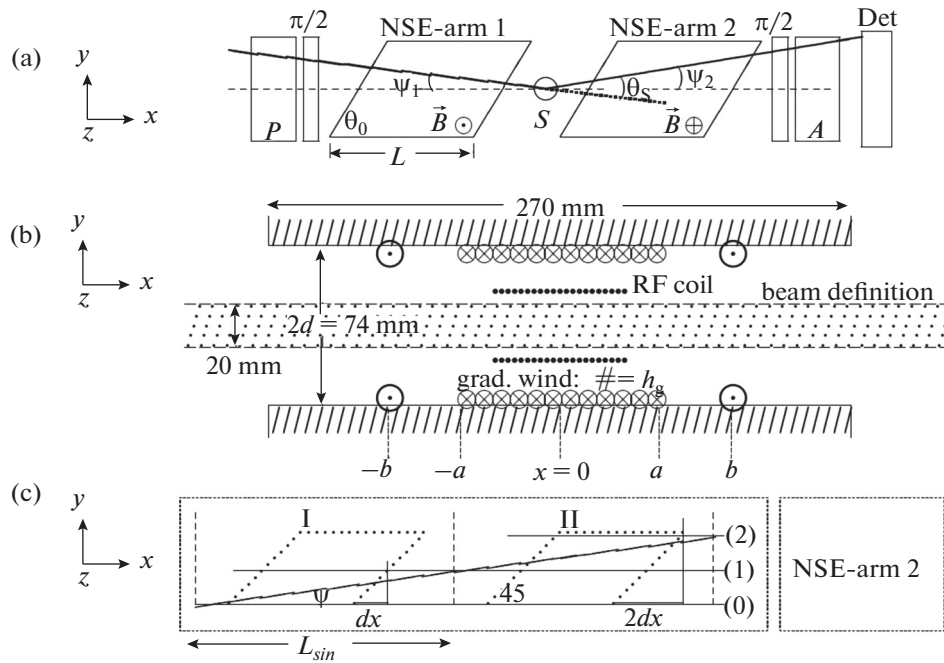
Fig. 1. (a) principle of SESANS [P = polariser, A = analyzer], (b) lay-out of the flipper for simulation, (c) illustrating how to model angle labeling. Notice: the coord.system for (b) is 90° rotated from (a) and (c).

ning δ means: repeat this, varying one of the parameters θ_0, L, B, λ over the range which the design of the setup allows. The polarisation $P(\delta)$ measured in this way contains information of the sample's properties Σ and $\frac{d\Sigma}{d\Omega}$ (total and differential macroscopic cross section). It is connected with the so-called "SESANS" correlation function $G(\delta)$ through

$$\frac{P(\delta)}{P_0(\delta)} = \exp(-\Sigma l[1 - G(\delta)])$$

$$\text{with } G(\delta) = \frac{1}{k_0^2 \Sigma} \iint \frac{d\Sigma}{d\Omega} \cos(Q_y \delta) dQ_y dQ_z, \quad (3)$$

l is the sample thickness; $k_0 = 2\pi/\lambda$ the neutron wavenumber. In general $G(\delta)$ is a function decaying from 1 at $\delta = 0$. We will not discuss it: a plethora of literature exists, see for example [4].

The denominator $P_0(\delta)$ is the polarisation of the empty setup when it is "focused" on spin-echo length δ. The **purpose of this article** is to find the *value* of $P_0(\delta)$ (which characterizes the quality of the setup) by simulation, in a variant with "adiabatic RF/gradient-flippers" [5], shown in Fig. 1b, c. We made MATLAB software [6] to simulate the Larmor precession in a NSE-arm made up of 2 such flippers and to calculate the coefficient Γ. *We use the 4 identical electro-magnets existing at PNPI*. We examine, if a SESANS setup with these flippers is a realistic option for PIK.

2. MAGNETIC FIELDS IN AN ADIABATIC RF/GRADIENT FLIPPER

The z-component $B_z^{DC}(x)$ of the **field of one DC magnet** was *measured* along its axis out to $x = \pm 28$ cm (Fig. 2). (We made no attempt to *calculate* the field from geometry). It has poles shaped as 45° parallelograms ($\theta_0 = 45°$). Outside the horizontal symmetry plane ($z \equiv 0$) there are x- and y-components. Following Ref [8], the x-component is calculated as follows: around the beam where no currents flow (current density $\mathbf{J} = \mathbf{0}$), the static Maxwell Equation $\text{rot}\mathbf{B} = \mu_0\mathbf{J}$ reduces to $\text{rot}\mathbf{B} = \mathbf{0}$. This implies among other:

$$\frac{dB_z(x)}{dx} - \frac{dB_x(z)}{dz} = 0 \rightarrow \frac{dB_z(x)}{dx} = \frac{dB_x(z)}{dz}.$$

Then the component B_x^{DC} at "height" z, expanded as:

$$B_x^{DC}(z) = B_x^{DC}(z = 0) + z\frac{dB_x^{DC}(z)}{dz}\bigg|_{z=0} + \ldots,$$

becomes, at any position x:

$$B_x^{DC}(z) = B_x^{DC}(z = 0) + z\frac{dB_z^{DC}(x)}{dx}\bigg|_{z=0} + \ldots.$$

Since in the horizontal symmetry plane ($z \equiv 0$) of the magnet the B_x^{DC} component is zero, we can drop the first term. The derivative $[dB^{DC}(x)/dx]_z = 0$ is found by numerically differentiating the measured $B^{DC}(x)$. Then, the x-component of the DC field along a trajec-
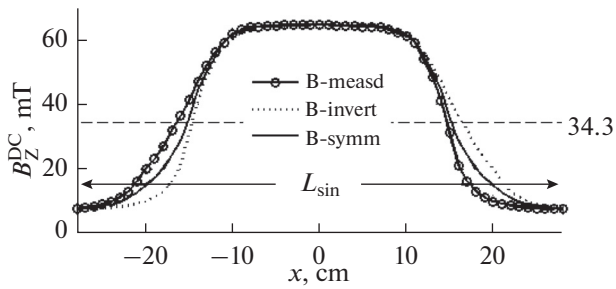
Fig. 2. Profile $B_z^{DC}(x)$ of the DC magnet measured along its axis at 5 A, variant after inverting in x and 'symmetrized' average. For the simulations $B_z^{DC}(x)$ is reduced such that the plateau is at 34.3 mT.

tory in the vertical symmetry plane ($y \equiv 0$) starting from ($x = -28$, z_0) at an angle ζ with the x-axis, is given by:

$$B_x^{DC}(x,z) = [z_0 + \zeta(x + 28)]\frac{dB_z^{DC}(x)}{dx}\bigg|_{z=0}. \qquad (4)$$

The **DC gradient field** $H_{gr}(x, z)$ is calculated (Biot and Savart) exactly from the lay-out of the windings in Fig. 1b. They are supposed to have infinite length in the y-direction. For the **RF field** $H_{RF}(x)$ along the axis we use the textbook formula for the field of a finite solenoid. To find $H_{RF}(x, z)$ with $z \neq 0$, an expansion simular to Eq. (4) is used.

The input used to calculate the fields for the simulation in Sec. **3** is listed in the caption of Fig. 3.

3. SIMULATION OF PRECESSION

We identify the *expectation values of the spin components along x, y, z* with the so-called "polarisation vector" $\mathbf{P}(t)$. In terms of this vector the Larmor Equation takes the familiar shape

$$\frac{d\mathbf{P}(t)}{dt} = \gamma \mathbf{P}(t) \times \mathbf{B}(t)$$

with $\gamma = 2\mu_n/\hbar$. For the simple case: homogeneous magnetic field **B** along z, this equation can be written as the (3×3) standard matrix $\Re_z$:

$$\mathbf{P}(t) = \Re_z(\alpha(t)) \times \mathbf{P}_{in}$$
$$\equiv \begin{pmatrix} \cos\alpha(t) & \sin\alpha(t) & 0 \\ -\sin\alpha(t) & \cos\alpha(t) & 0 \\ 0 & 0 & 1 \end{pmatrix} \mathbf{P}_{in}, \qquad (5)$$

where $\alpha(t)$ is the precession phase collected in the time that the field was acting on the vector **P**. For an arbitrary field **B** (defined by polar angle θ and azimuthal angle φ) Eq.(5) takes the form:

$$\mathbf{P}(t) = \Re_z(\varphi)\Re_y(\theta)\Re_z(\alpha(t))\Re_y^{-1}(\theta)\Re_z^{-1}(\varphi)\mathbf{P}_{in},$$

using the standard matrix $\Re_y$ for rotation around y.

For the simulation we follow the *Ansatz* taken for the first time in [7] (in a different context): we use a coordinate system, ROTATING about the field direction z of the DC magnet at the frequency ω_{RF} of the RF field. Seen in this system, a **constant virtual field**:

$$B^* = \gamma|\omega_{RF}|,$$
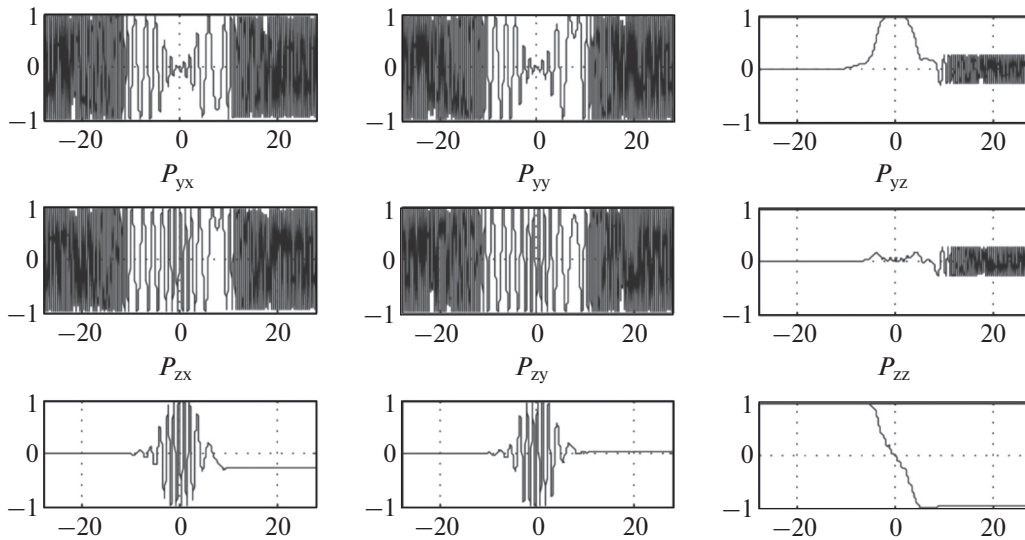
Fig. 3. Evolution of vectors [(100), (010), (001)] in the flipper Fig. 1b with *first guess parameters*: $N = 2000$, $\lambda = 6$ Å, $\omega_{RF} = 2\pi \times$ 1 MHz ($\rightarrow B^* = 34.3$ mT); **DC field**: B-measd in Fig. 2; **grad.wind**: number = n_g, a (Fig. 1b) = 46, $b = 80$ mm, curr = 4A; **RFcoil**: $R = 18$, $L = 60$ mm, wnd.dens.5/cm, curr = 4A.
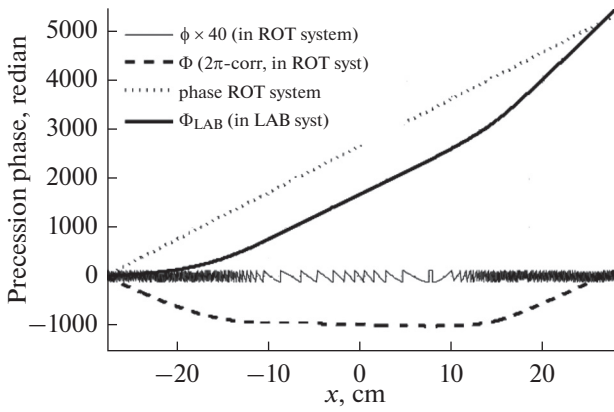
Fig. 4. Prec. phases through the flipper, with RF- and grad. current 4.0 A (ON). Parameters as in Fig. 3.

in the z-direction is "transformed away" (= subtracted from the actual field) over the full length L_{sim} in Fig. 2. Field components z − remain (diminished by B^*), but **stationary** components x- and y (the x- and y- components of the DC magnet- and the gradient field) rotate at $-\omega_{RF}$. It can be shown that these are ineffective on the vector **P**. The RF field is written as the sum of 2 fields (of half amplitude each) counter-rotating around z: one rotates at $-2\omega_{RF}$ (therefore also ineffective, making the RF field *half effective*); the other is stationary. We choose the phase of the ROT system such that close to the beam axis ($|y|, |z| < 1$ cm) the azimuthal angle φ of this latter field $= 0$ at any time, so the matrices $\Re_z(\varphi)$ and $\Re_z^{-1}(\varphi)$ in Eq. (6) reduce to the indentity matrix.

From the profile in Fig. 2 and the calculated gradient- and RF field (with *"first guess"* parameters in the caption Fig. 3) we can exactly calculate the field profiles of the flipper in the ROT system:

$$\Sigma A_z(x,y) = \mu_0 H_z^{gr}(x,z) + B_z^{DC}(x,y) - B^* \qquad (7)$$
(sum of the transverse components),

$$\Sigma A_x(x,y) = \mu_0 H_z^{RF}(x,z) \qquad (8)$$
(sum of the longitudinal components),

(ΣA_y vanishes because $\varphi = 0$). They span a field **A**(x, z) with absolute value $|A|(x, z)$, making a polar angle $\theta(x, z)$ with the z-axis. Ideally, this angle gradually increases as a function of x from 0 to π. The polarisation vector **P** will (roughly) "follow" the vector **A**(x, z) and "flip".

The length L_{sim} (see Fig. 2) of the measurement $B^{DC}(x)$ is divided into N steps of length dx_S. At the end of each step x_i ($-28 + dx_S < x_i < +28$ cm, $I = 1...N$), following Eq. (6), we calculate:

$$\mathbf{P}_{out,i} = \prod_{j=1}^{j=i} \Re_y(\theta_j) \Re_z(\alpha_j) \Re_y^{-1}(\theta_j) \mathbf{P}_{in} \equiv P^i \mathbf{P}_{in},$$

(so i is the upper boundary of the product Π), with inputs obtained from Eqs. (7, 8):

$$\theta_j = \tan^{-1}\left(\Sigma A_x(x_j, z)/\Sigma A_z(x_j, z)\right) \qquad (10)$$
(field orientation),

$$\alpha_j = (\gamma m_n/h)|A|(x_j, z)\lambda dx_S \qquad (11)$$
(precession phase),

N must be so high that $\alpha_j < \pi$ for all j. In the first step we take for $\mathbf{P}_{in}$ the vectors [(100), (010), (001)].

Figure 3 gives the result. To understand what happens, start with column 3. It shows the evolution for input polarisation (001). It is flipped at efficiency 0.95, but components along x and y appear. When the flipper is part of a SESANS setup, one prepares the vector (010) as input (by means of a $\pi/2$-flipper) at $x = -28$: column 2 gives the evolution. Installing also a $\pi/2$-flipper at $x = +28$ means: "measuring" P_{yy}. This element is set in a SESANS measurement in the setup of Fig. 1c.

Precession phase:

When the flipper is used in SESANS we must keep track of the precession phase. At the end of each step i, following the practice of 3D polarisation analysis, the collected phase ϕ_i of the vector **P** precessing around z is found by installing there (*in your mind*: it is practically impossible and we work in the ROT system) the equipment {$\pi/2$-flipper + anal + detec} and "measure" the elements $P_{yy}^i \approx \cos\phi_i$ and $P_{yx}^i \approx \sin\phi_i$. (Here, these elements have been *calculated* rather than measured).

Then, Eq. (5) suggests that the phase ϕ_i can be found, modulo 2π, by calculating

$$\phi_i \approx \tan^{-1}\left(P_{yx}^i/P_{yy}^i\right). \qquad (12)$$

The result, from the data P_{yx} and P_{yy} in Fig. 3, is plotted (for visibility multiplied by 40) in Fig. 4 as a shaky line. We made a MATLAB module to recover the multiples of 2π. Its output is plotted as the − line. *It is $\phi(x)$, seen in the ROT system.* The phase $\Phi_{LAB}(x)$ in the LAB system (thick full line) is found by adding the phase $\phi_{RF}(x) = \omega_{RF}(m_n/\hbar)\lambda x$ (dotted line) of the ROT system.

Precession phase through 2 flippers:

Next, we enter the vectors [(P_{xx}, P_{xy}, P_{xz}), (P_{yx}, P_{yy}, P_{yz}), (P_{zx}, P_{zy}, P_{zz})] at $x = 28$ as input for a second flipper, located 56 cm downstream. This means: we simulate a full NSE-arm made up of two flippers with centers 56 cm apart, over the beam length $2L_{sim}$. The precession phase $\Phi_{LAB}(x)$ through flipper II is added to the phase collected at the end $x = 28$ of flipper I.

It is plotted in Fig. 5 with flippers ON (RF&grad.curr = 4.0 A) and OFF (0.02 A). On approaching $x = 84$ the collected phase becomes constant, so it *can be measured in the LAB system* with the equipment {π/2-flipper + anal + detec}.

Between the flippers ($x = 12-44$ cm) with flippers ON, the slope is nearly twice the slope inside the flippers: this is "Zero Field Precession" (ZFP) [8] at frequeny $\simeq 2\omega_{RF}$. *So, the phase Φ_{LAB} collected in the NSE-arm can be made arbitrarily high, simply by putting flipper II farther behind flipper I.* This will not happen with flippers OFF (dotted lines), because then this slope is $\simeq 0$.

A divergent 2 cm heigh "ribbon beam":

We define a "ribbon beam" (in the vertical symmetry plane $y \equiv 0$) with a divergence such that all neutrons starting at $x = -28$, with z_0 between -1 and $+1$, remain until $x = 84$ inside the beam definition $|z| < 1$, sketched in Fig. 1b. Starting from ($x = -28, z_0 = 0$) this requirement means for the slope ζ in Eq. (4): $|\zeta| < 1/112$, so ζ must be in the interval $[-9...+9$ mr].

Starting from ($x = -28, z_0 = +1$) the interval is $[-18$ mr...0]; from ($x = -28, z_0 = -1$) it is $[0...+18$ mr].

This beam definition is mapped in Fig. 6: it is the area between the black lines. We introduce the weight factor $F(z_0, \zeta)$: $F = 1$ inside the beam definition and 0 elsewhere. By the step widths chosen, the full map is a grid of $21 \times 41 = 861$ paths $\{z_0, \zeta\}$; the area with $F = 1$ includes 441 paths. A simulation was done for all paths with $F = 1$. The phases $\Phi(x = 84, z_0, \zeta)$ using Eq. (12) and applying our module for the multiples of 2π are mapped as the *shaded pattern* in Fig. 6, after subtracting the phase found for the path $\{z_0 = 0, \zeta = 0\}$.

The *polarisation* of this beam, measured if {π/2-flipper + anal + det} were placed at $x = 84$, is the average of the *yy*-elements $P_{yy}^N(z_0, \zeta)$ of the matrices $P^N(z_0, \zeta)$ from Eq.(9) after flipper II:

$$P^N(z_0, \zeta) = \left[\prod_{j=1}^{j=N} R_y(\theta_j) R_z(\alpha_j) R_y^{-1}(\theta_j)\right]_{II}$$

$$\times \left[\prod_{j=1}^{j=N} R_y(\theta_j) R_z(\alpha_j) R_y^{-1}(\theta_j)\right]_I,$$

where the θ_j's and α_j's depend on the path $\{z_0, \zeta\}$. Then, the beam polarisation P_{yy} becomes:

$$P_{yy} \equiv \left\langle P_{yy}^N(z_0, \zeta)\right\rangle_{F=1}$$

$$= \frac{1}{441}\sum_{z_0=-1}^{1}\sum_{\zeta=-.01}^{+.01} F(z_0, \zeta)P_{yy}^N(z_0, \zeta). \quad (13)$$

To include the phasecoil (whose dimensions need not to be specified: at given λ it produces an extra precession $\Delta\phi$ around z for any neutron path) we must, for each
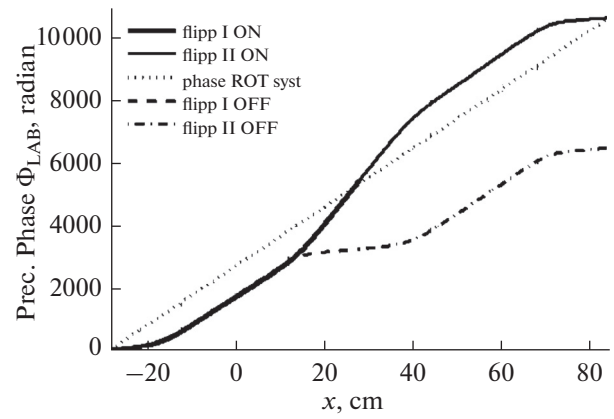
Fig. 5. Prec. phase $\Phi_{LAB}(x)$ through a NSE-arm of 2 flippers. The vertical lines mark the ends — projected on the symmetry axis ($y = 0, z = 0$) — of the parallellogram shaped DC magnet poles of flipper I and II.
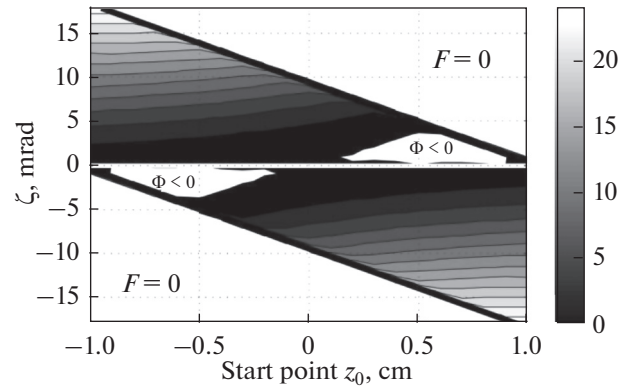
Fig. 6. Defining the parameters z_0 and ζ of the trajectories of a *divergent* ribbon beam: neutrons along a path with $\{z_0, \zeta\}$ *between the black lines* stay in the beam sketched in Fig.1b and will be detected. The *pattern* inside this region gives the final precession phases $\Phi(x = 84, z_0, \zeta)$ with flippers ON, $\lambda = 6$ Å.

path, multiply the matrix $P_{yy}^N(z_0, \zeta)$ by $R_z(\Delta\phi)$ and do the summation Eq.(13) for the *yy*-element of the product matrix. To simulate a sweep of the phasecoil through 2π, we repeat this for $\Delta\phi = i\pi/6$ ($i = 0...12$).

The dotted line in Fig. 7 is the signal $P_{yy}(\Delta\phi)$ thus found, when the averaging is limited to $\zeta = 0$. The amplitude is 1, so *flipper II cancels the phase spread after flipper I.* This is no longer true after averaging over the full area with $F = 1$: then the amplitude drops to 0.2 ($--$ line).

It is meaningless to show results obtained by Eq.(13) with flippers OFF, because in this case the amplitude of the phasecoil signal $P_{yy}(\Delta\phi)$ does not exceed 0.1.
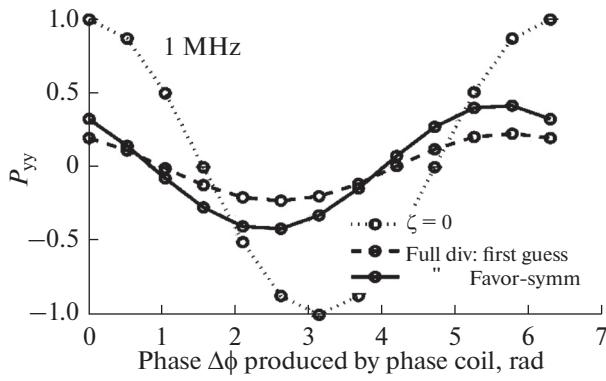
Fig. 7. Phasecoil signal $P_{yy}(\Delta\phi)$ for a NSE-arm composed of "first-guess" and favorite-symm flippers. Contrary to practice, these signals are undamped, because the simulation has no wavelength spread ($\lambda = 6$ Å).
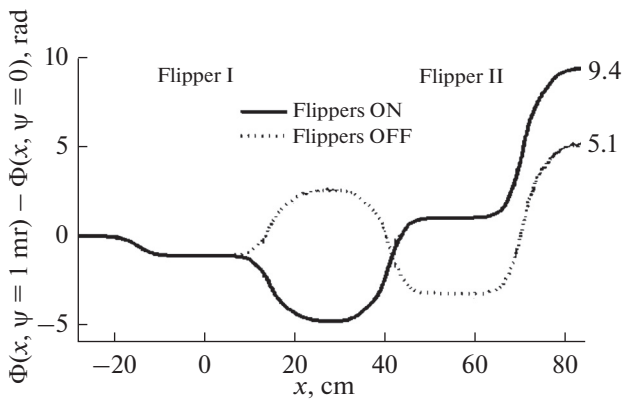
Fig. 8. Difference between precession phase ($\lambda = 6\,\text{Å}$) through the NSE-arm with *favorite-symmetric* flippers along 2 paths with {$z_0 = 0.4$, $\zeta = 0.004$}, but different "horizontal" directions: $\psi = 1$ mrad and $\psi = 0$.

Improving the flippers:

For input polarisation (001) after flipper I considerable elements P_{xz} and P_{yz} appear (Fig. 3-col.3). In simulations with 2 flippers in general they grow in flipper II. By varying input parameters we tried to reduce these elements and to improve other properties of the flippers. This has lead to the so-called "*favorite-symmetric*" flipper, obtained from the *first-guess* flipper (caption Fig. 3) by:

(1) extending and increasing the gradient field [set numb.windings n_g 24 → 28, a (Fig. 1b) 46 → 54, b 80 → 96 mm; current 4 → 5 A] to reduce x and y components;

(2) "constructing" an idealized DC magnet [take the symmetrized profile for $B_z^{DC}(x)$ (see Fig. 2) instead of the profile *as measured*] to reduce the spread in precession phase after the flipper;

(3) reducing RF current from 4 → 1.5 A to minimize the required RF power.

The phasecoil signal $P_{yy}(\Delta\phi)$ according to Eq.(13) for the NSE-arm made up of such improved flippers is shown in Fig. 7 as a full line. The amplitude of the signal grows from 0.2 to 0.4.

4. FiNDiNG THE LABELING COEFFICIENT

The field profiles $B_z^I(x, z_0)$ and $B_z^{II}(x, z_0)$ in flippers I and II along a path ∥ the plane $z \equiv 0$ at an angle $\psi \neq 0$ with the x-axis can be found from the profile in Fig. 2. **Profile** B_z^I is a transition from $B_z^{(0)}(x, z_0) \equiv B_z^{DC}(x)$ along path (0) to $B_z^{(1)}(x, z_0)$ along path (1). Given that the magnet poles are 180 mm wide in the y-direction, we suppose that $B_z^{(1)}(x, z_0) = B_z^{DC}(x + dx, z_0)$; the shift dx is

$$dx(\psi) = \psi L_{sim}\cot(45°) \quad (14)$$
$$(dx:\text{ see Fig.1c; } L_{sim}:\text{ see Fig.2}).$$

Profile B_z^{II} is a transition from $B_z^{(1)}(x, z_0) = B_z^{DC}(x + dx, z_0)$ along path (1) to $B_z^{(2)}(x, z_0) = B_z^{DC}(x + 2dx, z_0)$ along path (2). Describing these transitions with the parameter $\varepsilon(x)$ running linearly from 0 to 1 over L_{sim}, we get — with $dx(\psi)$ given by Eq. (14):

$$\begin{aligned} B_z^I(x, z) &= (1 - \varepsilon)B_z^{DC}(x, z) \\ &+ \varepsilon B_z^{DC}(x + dx(\psi), z), \end{aligned} \quad (15)$$

$$\begin{aligned} B_z^{II}(x, z) &= (1 - \varepsilon)B_z^{DC}(x + dx(\psi), z) \\ &+ \varepsilon B_z^{DC}(x + 2dx(\psi), z). \end{aligned} \quad (16)$$

These expressions remain valid for paths with $\zeta \neq 0$.

We calculated the precession phase through a NSE-arm with 2 *favorite-symmetric* flippers for $\psi = 1$ mrad and $\psi = 0$, for an arbitrary set {z_0, ζ}. The difference is plotted in Fig. 8. At right the term $\lambda\Gamma$ ($\lambda = 6$ Å) in Eq. (1) is indicated. This implies for a SESANS experiment at $\lambda = 6$ Å with the setup in Fig. 1c this implies: *1 mrad deviation in a scattering process in a sample behind the NSE-arm will give* $\Delta\Phi = 9.4$ [5.1] **rad** *more precession for the scattered beam through a second similar NSE-arm.*

Hence, the **labeling coefficient** Γ with flippers ON[OFF] is 1.57[0.85] $\times 10^3$ Å^{-1}.

Dependence empty beam polarisation on spin-echo length δ:

For $\lambda = 2$–10 Å we constructed the phasecoil signals $P_{yy}(\Delta\phi)$ according to Eq. (13) and determined

their amplitudes A. In the introduction we identified $A(\lambda)$ with the empty beam polarisation $P_0(\lambda)$.

Using Eq.(2) and the result for Γ of the previous subsection, the wavelength λ [in Å] can be converted to spin-echo length δ [in μm] according to:

$$\delta(\lambda) = 0.1 \frac{1.57[0.85]}{2\pi} \lambda^2 \quad \text{(flippers ON[OFF]),}$$

to get P_0 as a function of δ. The result (flippers ON) is shown in Fig. 9.

This result was obtained in the ROT system. To transform it to the LAB system, for each λ, for all paths, the matrix $P^N(z_0, \zeta)$ in Eq. (13) must be "rotated forward" around z, over an angle equal to the phase $\phi_{RF}^N(x) = \omega_{RF}(m_n/h)\lambda x_N$ attained by the ROT system at $x_N = 84$ (equal for all paths). This is done by inserting the matrix $R_z(\phi_{RF}^N)$ under the Σ-signs. The *phase* of the signals $P_{yy}(\Delta\phi)$ will shift compared with their appearance in Fig. 7, but their *amplitude* is practically unchanged. So, Fig. 9 is also valid in the LAB system.

In similar way one can compensate the phase collected along the path $(0,0)$: insert under the Σ-signs in Eq.(13) the inverse of the matrix $P^N(z_0 = 0, \zeta = 0)$. This will give another shift of the phasecoil signals $P_{yy}(\Delta\phi)$ but not change their amplitude. Then, Fig. 9 can be interpreted as the result of an empty-beam NSE-experiment in which NSE-arm 2 compensates *the phase collected along path* $(0,0)$ *through arm 1*, for any path. In this interpretation arm 2 is an "infinite" coil with homogeneous field $\parallel z$ over the full beam cross section, without angle labeling term.

The way presented in Fig. 9 refers to a SESANS setup in a "white" neutron beam, with TOF data collection. However, this calculation can also be done at fixed λ and varying ω_{RF}.

5. DISCUSSION AND CONCLUSION

The first order approach Eq. (4) for the field of the DC magnet gives errors, increasing with $|z|$. To estimate them, we exactly calculated the *field components* B_z and B_x and the *precession* in a model magnet, consisting of "line poles" above and below the plane $z \equiv 0$, with parameters chosen such that the profile $B_z(x, z = 0)$ is very similar to Fig. 2. The calculation was repeated using the approach Eq. (4). For $|z| < 1$ cm the differences are so small that we can ignore the errors due to the first order approach; for $|z| > 1$ they increase rapidly.

Subtracting the precession phase for the path $\{z_0 = 0, \zeta = 0\}$ means physically that NSE-arm 1 is put in echo with a second arm *without the property of angle labeling*. To make the simulation more realistic, it is
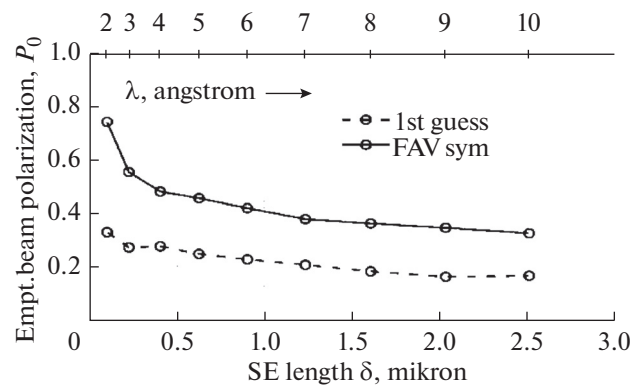
Fig. 9. Empty beam polarisation $P_0(\delta)$ for a SESANS setup, traversed by the *ribbon beam* of Fig. 6: **NSE-arm 1** is composed of 2 adiab RF/gradient flippers [operated at RF = 1 MHz] with centers 56 cm apart; **NSE-arm 2** is a hypothetical infinite coil giving equal precession phase for all neutron paths.

needed to replace it with an arm equal to arm 1. Then, the spread in precession phase mapped in Fig. 6 will be *partially, not fully* corrected by arm 2. Hence, the amplitudes of the phasecoil signals in Fig. 9 are pessimistic.

The routines developed for this simulation are a way to simulate Larmor precession in a non-trivial magnetic field configuration for neutron paths at angles $\zeta, \psi \neq 0$ from the beam axis. By the first order approach for the field, no full map of the magnetic field is required.

Comparing the results (Figs. 7 and 9) for the DC magnet without/with symmetrized field (Fig. 2) makes clear that the symmetry of this magnet is decisive for the amplitude of the phasecoil signal of the SESANS setup. This can be easily achieved by mounting them carefully.

The values for δ in Fig. 9 are below our wishes. Remember: the final phase in each NSE-arm can be increased by putting the flippers (for example) a factor 5 further apart (at the cost of intensity); also: on basis of the experience reported in [5], RF frequency ω_{RF} of $2-3$ MHz looks possible. Both options are the subject of our present simulations. They give an outlook to $\delta \simeq 20$ μm.

The routines developed for this simulation are a way to simulate Larmor precession in a non-trivial magnetic field configuration for neutron paths at angles $\zeta, \psi \neq 0$ from the beam axis. By the first order approach for the field, no full map of the magnetic field is required. This work could be of value in the design of similar installations elsewhere, for example OFFSPEC at ISIS [11].

We conclude: the results are sufficiently realistic to claim that a SESANS setup at PIK based on the available magnets is a realistic option.

REFERENCES

1. W. H. Bouwman, W. H. Kraan, and M. T. Rekveldt, Phys. B **267−68**, 79−83 (1999).

2. Roger Pynn, M. R. Fitzsimmons, W. T. Lee, V. R. Shah, A. L. Washington, P. Stonaha, and Ken Littrell, J. Appl. Crystallogr. **41**, 897−905 (2008).

3. M. Th. Rekveldt, J. Plomp, W. G. Bouwman, W. H. Kraan, S. V. Grigoriev, and M. Blaauw, Rev. Sci. Instrum. **76**, 033901 (2005).

4. W. H. Kraan, V. N. Zabenkin, Yu. O. Chetverikov, M. Th. Rekveldt, C. P. Duif, and S. V. Grigoriev, Phys. B **397**, 79−81 (2007).

5. A. A. Sumbatyan, V. N. Slusar, A. I. Okorokov, and H. Eckerlebe, Instrum. Exp. Tech. **52**, 337 (2009).

6. W. H. Kraan, et al., J. Surf. Invest.: X-ray, Synchrotron Neutron Tech. **8** (5), 1035−1043 (2014).

7. W.H.Kraan@tudelft.nl.

8. O. Uca, W. H. Kraan, W. G. Bouwman, and M. T. Rekveldt, Phys. B **297** (1), 28−31 (2001).

9. A. Abragam, *Principles of Nuclear Magnetism* (Oxford Univ. Press, New York, 1961).

10. R. Gähler and R. Golub, J. Phys. (Paris) **49**, 1195 (1988).

11. R. M. Dalgliesh, S. Langridge, J. Plomp, V. O. De Haan, and A. A. Van Well, Phys. B **406** (12), 2346−2349 (2011).

SPELL: 1. OK